# Damping of field-induced chemical potential oscillations in ideal two-band compensated metals

Jean-Yves Fortin, Alain Audouard

# Damping of field-induced chemical potential oscillations in ideal two-band compensated metals

Jean-Yves Fortin[1*] and Alain Audouard[2†]
[1]*Laboratoire de Physique Théorique, Université Louis Pasteur (UMR CNRS-ULP 7085), 3 rue de l'Université, F-67084 Strasbourg cedex, France*
[2]*Laboratoire National des Champs Magnétiques Pulsés (UMR CNRS-UPS-INSA 5147) 143 avenue de Rangueil, F-31400 Toulouse, France*
(Dated: April 1, 2008)

The field and temperature dependence of the de Haas-van Alphen oscillations spectrum is studied for an ideal two-dimensional compensated metal. It is shown that the chemical potential oscillations, involved in the frequency combinations observed in the case of uncompensated orbits, are strongly damped and can even be suppressed when the effective masses of the electron- and hole-type orbits are the same. When magnetic breakdown between bands occurs, this damping is even more pronounced and the Lifshits-Kosevich formalism accounts for the data in a wide field range.

PACS numbers: 71.18.+y,71.20.Rv,74.70.Kn



## I. INTRODUCTION

In large enough magnetic field, the Fermi surface (FS) of multiband quasi-two-dimensional metals, is liable to give rise to networks of orbits coupled by magnetic breakdown (MB). The most studied type of network is the linear chain of coupled orbits introduced by Pippard[1] and illustrated by several quasi-two-dimensional (q-2D) organic conductors such as $\kappa$-(BEDT-TTF)$_2$Cu(NCS)$_2$. As discussed, in Ref.[2], magnetic oscillations spectra of such networks contain many frequencies that are linear combinations of two basic frequencies. In addition to those linked to MB-induced orbits, other frequencies are observed that are not accounted for by the semi-classical theory of Falicov and Stachowiak[3]. They can be attributed to quantum interference (as far as magnetoresistance oscillations are concerned), MB-induced modulation of the density of states[4–6] and oscillation of the chemical potential[7–10], even though the actual respective contribution of these three phenomena to the oscillatory behavior remains to be established.

Another type of network is provided by q-2D metals of which the FS is composed of compensated electron- and hole-types tubes. This is the case of the family of organic metals (BEDT-TTF)$_8$Hg$_4$Cl$_{12}$(C$_6$H$_5$X)$_2$ (X = Cl, Br) whose FS, which originates from two pairs of crossing q-1D sheets, is composed of one electron and one hole tube with the same area[11]. As it is the case of the above-mentioned linear chains of coupled orbits, magnetoresistance oscillations spectra in this type of network reveal frequencies that are linear combinations of three basic frequencies, linked to the compensated orbits and to the two FS pieces located in-between[12–14]. However, in striking contrast to the data relevant to linear chains of orbits, de Haas-van Alphen (dHvA) oscillations spectra recorded in the case of the compound with X = Br only exhibit oscillations, the field and temperature dependence of which can be consistently interpreted on the basis of the semiclassical model of Falicov and Stachowiak[3,14]. Analogous networks are observed in organic metals, with two carriers per unit cell. In this case, the FS originates from the overlapping in two directions of hole tubes with an area equal to that of the First Brillouin zone (FBZ) and from the resulting gap openings[15]. As reported in the case of (BEDO)$_4$Ni(CN)$_4$·4CH$_3$CN[16], such a FS yields a network consisting in two hole- and one electron-type tubes (see Fig. 1(a)). Closely related network is obtained in the case where the large hole orbit come close to the FBZ boundary, as it is the case of (BEDT-TTF)$_4$NH$_4$[Fe(C$_2$O$_4$)$_3$][17]. In this latter case, a large MB gap is observed at this point and the resulting network only consists in one electron- and one hole-type orbit, as displayed in Fig. 1(b). Linear chain of successive electron-hole tubes might also be observed in Bechgaard salt (TMTSF)$_2$NO$_3$[18,19].

The aim of this paper is to explore the field and temperature dependence of the dHvA oscillations spectra of an ideal 2D metal whose FS is composed of one electron- and one hole-type compensated orbit. It is demonstrated that the field-induced oscillations of the chemical potential are strongly damped for such a FS and can even be suppressed in the case where electron- and hole-type orbits have the same effective masses. The chemical potential oscillations can be even more damped when the two orbits are coupled by MB. In this case, the Lifshits-Kosevich (LK) formalism accounts for the data up to high magnetic field and low temperature.

## II. MODEL

We first consider a 2D metal whose electronic structure consists of two parabolic bands of hole- and electron-type, respectively. The bottom of the electron band is set at zero energy while the top of the hole band is at $\Delta > 0$. The total number of electrons in the system is such that the hole band is completely filled. Since the lower part of the electron band is lower in energy than the top of the hole band, some quasiparticles move to the electron band

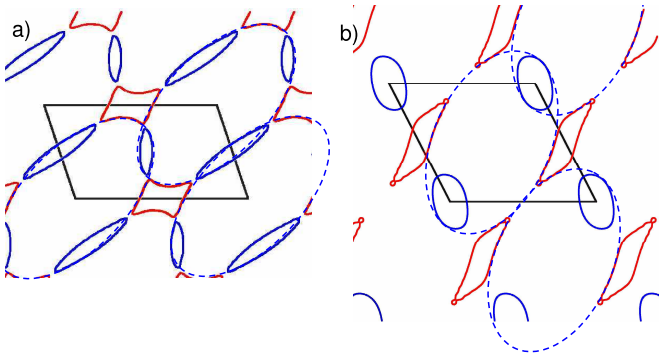


FIG. 1: (color online) Calculated Fermi surface (FS) of q-2D organic metals (a) $(BEDO)_4Ni(CN)_4{\cdot}4CH_3CN$[16] and (b) $(BEDT\text{-}TTF)_4NH_4[Fe(C_2O_4)_3]$[17] leading to networks of compensated electron- and hole-orbits (solid red and blue lines, respectively). Ellipses in dotted blue lines correspond to the hole orbits, with an area equal to that of the FBZ, from which the FS is built (see text).

in order to lower the total energy. The effective masses linked to the two bands, $m_e^* \equiv 1/C_e$ and $m_h^* \equiv 1/C_h > 0$, can be different. It is useful to define the physical units of the problem. The reduced field $b = eB\mathcal{A}_0/h$ is in units of the characteristic field $\tilde{B} = h/e\mathcal{A}_0$, the effective masses are in units of the electron mass $m_e$, the energies are in units of $\tilde{E} = 2\pi\hbar^2/m_e\mathcal{A}_0$ and the temperature $t$ in units of $\tilde{T} = \tilde{E}/k_B$. Given a unit cell area $\mathcal{A}_0$ =197.6 Å$^2$, which stands for $(BEDT\text{-}TTF)_8Hg_4Cl_{12}(C_6H_5Cl)_2$[20], we obtain $\tilde{B}$ = 2093 T and $\tilde{T}$ = 2812 K. Therefore, realistic experimental conditions yield small values of $b$ and $t$ compared to $\tilde{B}$ and $\tilde{T}$, respectively. The semi-classical quantization of the energy levels in the presence of a magnetic field leads to the Landau equations:

$$E_e(n) = C_e b(n+\frac{1}{2}), \quad E_h(n) = \Delta - C_h b(n+\frac{1}{2}) \qquad (1)$$

each Landau level (LL) having a degeneracy $b$ per sample area. The zero field Fermi energy is simply given by $E_F = m_h^*/(m_e^*+m_h^*)\Delta$. At finite temperature, the total free energy is given by the difference between the contribution of the electron and of the hole band, with the condition that the total number of quasiparticles $N_{eh}$ is fixed. In addition, the compensation condition imposes that the number of quasiparticles in the electron ($N_e$) and in the hole ($N_h$) band are the same. From the thermodynamical relations, we can define a free energy for the system based on the difference between the free energy for the electrons in the electron band and the free energy for the holes in the hole band $\Delta F = \Omega_e - \Omega_h + (N_e - N_h)\mu$, where $\Omega_{e(h)}$ is the Grand Potential for the electrons (holes) and $\mu$ is the chemical potential [$\mu(t=0,b) = E_F(b)$]:

$$\begin{aligned}\Omega_e(t,b) &= -tb\sum_{n\geq 0}\log\left(1+\exp[\beta(\mu - E_e(n))]\right)\\ \Omega_h(t,b) &= tb\sum_{n\geq 0}\log\left(1+\exp[\beta(E_h(n) - \mu)]\right) \qquad (2)\end{aligned}$$

Since $N_e = N_h$, we conclude that $F = \Omega_e - \Omega_h$ in compensated metals. $\mu$ is evaluated from the self-consistent equation $\partial\Delta F/\partial\mu = 0$. At zero temperature, the above expressions reduce simply to the ground state (GS) energy $\Delta E_0$. The Fermi energy $E_F(b)$ is given by the condition $n_e b = n_h b$, where $n_e$ and $n_h$ are the (integer) numbers of LL filled, and

$$\begin{aligned}\Delta E_0 &= -b\sum_{n=0}^{n_e-1}(E_F(b) - E_e(n)) - b\sum_{n=0}^{n_h-1}(E_h(n) - E_F(b))\\ &= E_e - E_h + b(n_h - n_e)E_F(b) = E_e - E_h \qquad (3)\end{aligned}$$

The special cases where the Fermi energy goes trough one Landau level, or where this Landau level is partially filled, correspond to singular points in the energy spectrum as a function of the inverse field that do not modify the thermodynamical quantities. The exact expression for $\Delta E_0$ is simply

$$\Delta E_0 = \frac{1}{2}(C_e + C_h)b^2 n_e^2 - b\Delta n_e \qquad (4)$$

with $n_e = [E_F/C_e b + 1/2]_i$, the notation $[.]_i$ standing for the integer part of the argument. The GS energy oscillates around the limit of zero field, where $\Delta E_0(q=1) = -\Delta^2/2(C_e+C_h)$. For example, taking $\Delta = 1$, $C_e = 1$ and $C_h = 2/5$, we obtain $\Delta E_0 \simeq -0.357$. We deduce the oscillating part of the magnetization $M_{osc} = -\partial\Delta E_0/\partial b$ from the latter expression, using succesively the Fourier transforms of the periodic functions $[x]_i - x$ and $([x]_i - x)^2$:

$$M_{osc} = -(C_e + C_h)F_0\sum_{k\geq 1}\frac{(-1)^k}{\pi k}\sin(2\pi k F_0/b) \qquad (5)$$

where $F_0 = \Delta/(C_e+C_h) = m_e^* m_h^*\Delta/(m_e^*+m_h^*)$ is the fundamental frequency corresponding to the FS area of the electron and hole band. At zero temperature and for fixed number of electrons, the magnetization oscillates with characteristic frequency $F_0$, and the amplitudes $A_k$ of the $k^{th}$ harmonics are given by the LK formula with $1/k$ dependence[21]:

$$A_k = (-1)^{k+1}\frac{F_0}{k\pi}(C_e + C_h) \qquad (6)$$

The sum $C_e + C_h$ means that the 2 orbits circulating around the hole and electron bands contribute individually to the magnetization.

## III. SELF-CONSISTENT EQUATION FOR THE CHEMICAL POTENTIAL

The oscillatory parts of the Grand Potentials Eqs. (2) can be extracted using Poisson's formula for any function $F(x)$ (see Ref.[21,22] for details):

$$\frac{1}{2}F(0)+\sum_{n\geq 1}F(n)=\int_0^\infty F(x)dx + 2\Re\sum_{n\geq 1}\int_0^\infty F(x)\exp(2i\pi nx)dx \quad (7)$$

where $F(n)$ is equal to $\log(1+\exp[\beta(\mu-E_e(n))])$ or $\log(1+\exp[\beta(E_h(n)-\mu)])$ for electrons and holes, respectively. The last series in Eq. (7) gives the oscillatory part of the Grand Potential in terms of Fourier components. The index $n$ is expressed as a function of the energy $n=n(E)$ by relations (1), then expanded around the chemical potential $\mu$ at low temperature where the energy derivatives of the distribution functions $1/(1+\exp[\beta(E_e(n)-\mu)])$ or $1/(1+\exp[\beta(\mu-E_h(n))])$ are strongly peaked. After some algebra, we obtain for each band

$$\Omega_e \simeq -\frac{1}{2C_e}\mu^2 + \frac{b^2C_e}{2}\left[\frac{1}{12}+\sum_{n=1}^{\infty}\frac{(-1)^n}{\pi^2n^2}R(nm_e^*)\cos(2\pi n\frac{\mu}{C_eb})\right] \quad (8)$$

$$\Omega_h \simeq \frac{1}{2C_h}(\Delta-\mu)^2 - \frac{b^2C_h}{2}\left[\frac{1}{12}+\sum_{n=1}^{\infty}\frac{(-1)^n}{\pi^2n^2}R(nm_h^*)\cos(2\pi n\frac{\Delta-\mu}{C_hb})\right] \quad (9)$$

where

$$R(nm^*_{e(h)})=\frac{2\pi^2nm^*_{e(h)}t/b}{\sinh(2\pi^2nm^*_{e(h)}t/b)} \quad (10)$$

is the temperature reduction factor for effective masses $nm^*_{e(h)}$. A Dingle term $R_D(nm^*_{e(h)},t^*_{e(h)})=\exp(-2\pi^2nm^*_{e(h)}t^*_{e(h)}/b)$ can also be added in the case where the relaxation times $t_e^*$ and $t_h^*$ for electron- and hole-band have to be taken into account. In the following we will assume that these two relaxation times are negligible for convenient purpose. It is always possible to add those terms in final expressions. The chemical potential satisfies therefore the self-consistent relation:

$$\mu = E_F + \frac{b}{m_e^*+m_h^*}\sum_{n=1}^{\infty}\frac{(-1)^n}{\pi n}[R(nm_h^*)\sin(2\pi n\frac{\Delta-\mu}{C_hb}) - R(nm_e^*)\sin(2\pi n\frac{\mu}{C_eb})] \quad (11)$$

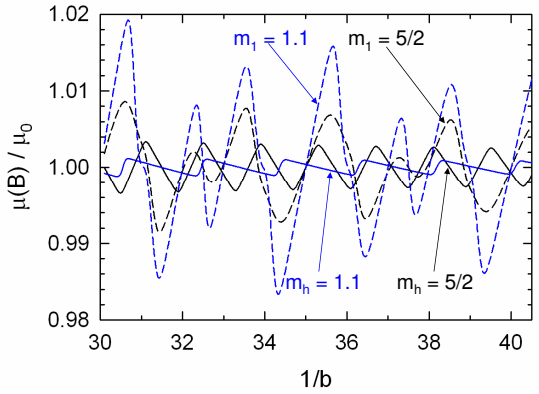


FIG. 2: (color online) Field dependence of the chemical potential normalized to its value in zero-field at t = 0.001. Solid and dashed lines correspond to one electron and one hole compensated orbits (with $m_e^*=1$ and $m_h^*=1.1$ or 5/2) and two electron orbits (with $m_0^*=1$ and $m_1^*=1.1$ or 5/2), respectively (see text).

At a first order approximation, which will be discussed in the following sections, we can replace $\mu$ in the sine functions of the previous expression by $E_F$ when the oscillations of the chemical potential are small compared to $E_F$, in the small field and high temperature regime ($t/b$ large). This gives:

$$\mu \simeq E_F + \frac{b}{m_e^*+m_h^*}\times \sum_{n=1}^{\infty}\frac{(-1)^n}{\pi n}[R(nm_h^*)-R(nm_e^*)]\sin(2\pi n\frac{F_0}{b}) \quad (12)$$

It can be remarked first that, in the case where the effective masses and relaxation times linked to the electron- and hole-type orbits are the same, there is an exact solution for Eq. (11) with $\mu=E_F$. In this case the oscillatory part of Eq. (11) or Eq. (12) vanishes and the chemical potential remains constant in magnetic field and temperature. This is due to the fact that the energy levels are symmetric around $E_F$. More generally, the amplitude of the chemical potential oscillations can be compared to the case of two electron bands[10]. In Fig. 2, the field-dependent chemical potential Eq. (11) is calculated for compensated orbits with $m_e^*=1$ and $m_h^*=1.1$ or 5/2 and compared to the case of two electronic orbits with effective masses $m_0^*=1$ and $m_1^*=1.1$ or 5/2. It can be observed that the chemical potential oscillations are strongly damped for compensated orbits, even in the case where $m_h^*$ and $m_e^*$ have strongly different values[23].

## IV. DE HAAS-VAN ALPHEN OSCILLATIONS

The oscillatory magnetization can be obtained putting the solution of the chemical potential given by Eq. (11)

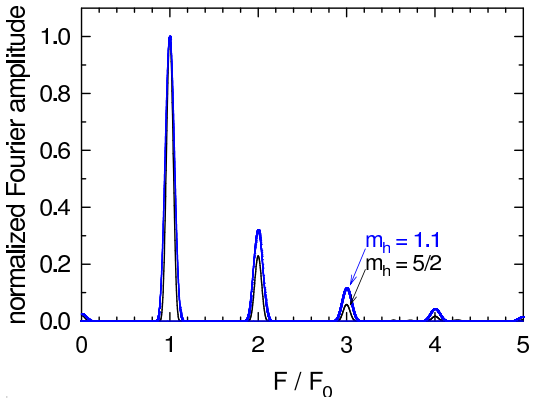


FIG. 3: (color online) Fourier spectrum of the magnetization at t = 0.001 for $m_e^* = 1$ and $m_h^* = 1.1$ or 5/2. The field range is from b = 0.015 to b = 0.033. $F_0$ is the fundamental frequency (see text).

back into the expression for the free energy $F$ using Eqs. (1) and (2). As discussed above, the chemical potential is field-independent for $m_e = m_h$ and the LK formula[21] holds in this case. However, for $m_e^* \neq m_h^*$, the oscillatory magnetization differs from the LK theory. Examples of Fourier analysis of the magnetization are given in Fig. 3. It should be noted that, contrary to the case of electron-hole systems away from exact compensation[24], frequency combinations are not observed directly in the oscillatory spectra. However, as discussed later on, deviations from the LK behavior are observed for the second harmonics.

It is useful for experimentalists, to check to what extent it is possible to determine a temperature and field range in which the LK formalism provides a satisfactory approximation of the oscillatory behavior in the case where $m_e^* \neq m_h^*$. The b/t dependence of the Fourier components of the magnetization with frequencies $F_0$ and $2F_0$ are given in Fig. 4. The LK formula accounts for the field and temperature dependence of the first harmonics. Furthermore, it can be noticed that in the case where $m_h^*$ is strongly different from $m_e^*$, the contribution of the orbit with the smallest effective mass dominates in a large field range (see the dashed line in Fig. 4a). It has also been checked that, in the opposite case where $m_e^*$ is close to $m_h^*$, the data can be accounted for by the contribution of only one orbit with a mean effective mass, namely, $m_{mean}^* \simeq (m_e^* + m_h^*)/2$. In contrast, the LK formula cannot account for the second harmonics in the case where $m_e^*$ and $m_h^*$ significantly differ. The observed behavior of the second harmonics in this latter case is reminiscent to that observed for two electronic orbits[10].

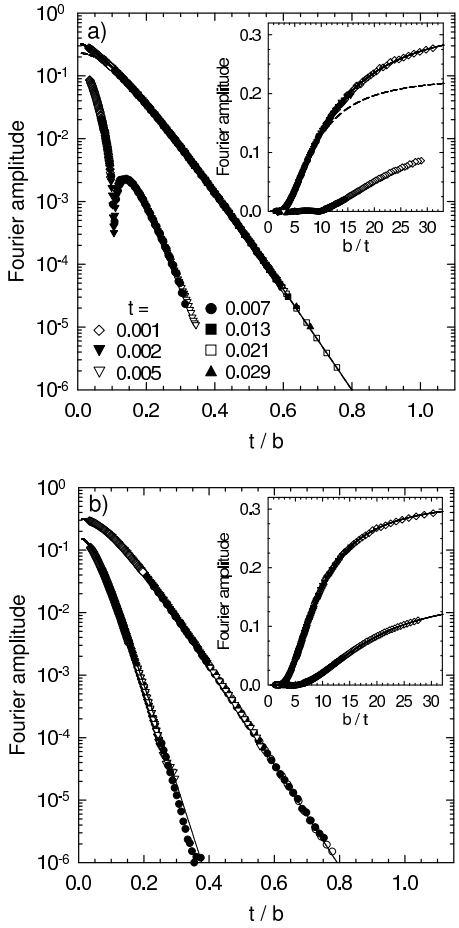


FIG. 4: t/b dependence of the Fourier components of the magnetization with frequencies $F_0$ and $2F_0$. The effective mass of the electronic-type orbit is $m_e^* = 1$. The effective mass of the hole-type orbit is $m_h^* = 5/2$ and 1.1 in (a) and (b), respectively. Solid lines are obtained from the LK formula. The dashed line in (a) corresponds to the contribution of the electronic orbit, only.

## V. MAGNETIC BREAKDOWN

In this section, we consider the case where the magnetic field is large enough for the quasiparticles can tunnel through MB between the two bands.

The topology of the new FS is depicted in Fig. 5: the quasiparticles can tunnel between the junctions $\alpha'$ and $\beta$ ($\beta'$ and $\alpha$) with probability amplitude $ip$ or be reflected between the junctions $\alpha'$ and $\alpha$ ($\beta'$ and $\beta$ respectively) with probability amplitude $q$. This surface is a simplification of Fig. 1b in the sense that it does not include the 1D network feature. $p$ and $q$ are related by $p^2 + q^2 = 1$[3,21], and the field dependence of $p$ is given by the Chambers formula $p = \exp(-b_0/2b)$[25,26], where $b_0$ is a characteristic MB field. $b_0$ comes in the field range covered by experiments in the case where the two bands are located closely enough in the FBZ. Depending on the band type (electron or hole), the quasiparticle wavefunction acquires a phase either $\sigma_e = S_e/b$ or $\sigma_h = S_h/b$

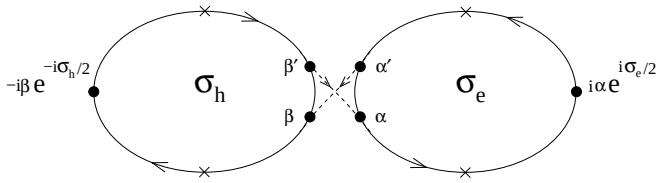


FIG. 5: Fermi surface of a two-band model with magnetic breakdown in the FBZ. The quasiparticles orbit clockwise for the Hole surface and counterclockwise for the Electron band. They can tunnel between the points (which represent also the amplitudes of the wave-function) $\alpha'$ and $\beta$ (or $\beta'$ and $\alpha$) with a probability amplitude $ip$, or be relected between $\alpha'$ and $\alpha$ (or $\beta'$ and $\beta$) with a probability amplitude $q$. At the turning points (cross symbols), the wavefunction acquires a factor $i$ (or $-i$) depending wether the quasiparticle orbits an electron or hole surface.

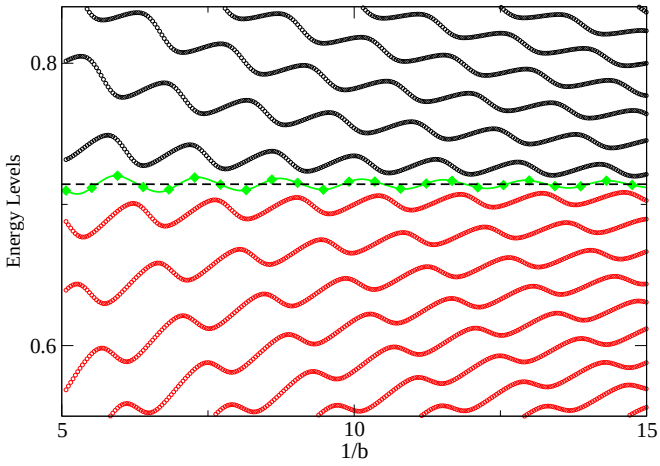


FIG. 6: (color online) Energy levels for a reflection amplitude $q = 0.6$ (or, equivalently, tunnelling amplitude $p = \sqrt{1-q^2}$), $\Delta = 1$, $m_e^* = 1$ and $m_h^* = 5/2$. Levels that belong to a quasi-electron band (going upwards in the limit of large field, black lines) above the Fermi energy $E_F(b)$ (diamond symbols, green line) can be distinguished from levels that belong to a quasi-hole band (respectively going downwards, red lines). The Fermi energy at zero field is shown as a dashed line.

when orbiting around each part of the Fermi surface (between $\alpha$ and $\alpha'$ counterclockwise for the electron band or $\beta$ and $\beta'$ clockwise for the hole band). The semiclassical actions $S_e = 2\pi m_e^* E$ and $S_h = 2\pi m_h^*(\Delta - E)$ represent the areas delimited by each Fermi surface in the FBZ. Assuming that the wavefunction of the quasiparticle is $\alpha$ at the point $\alpha$, we obtain that after one orbit around the electron band, $\alpha' = -\alpha \exp(i\sigma_e)$ (the quasiparticle goes through 2 turning points where it acquires a factor $i$ or $-i$ each time, depending on the electron or hole type[26]). Similarly, it follows $\beta' = -\beta \exp(-i\sigma_h)$ for the hole band. The four amplitudes $\alpha$, $\alpha'$, $\beta$ and $\beta'$ are related by the transfer matrix[5,26]

$$\begin{pmatrix} \alpha \\ \beta \end{pmatrix} = \begin{pmatrix} q & ip \\ ip & q \end{pmatrix} \begin{pmatrix} \alpha' \\ \beta' \end{pmatrix} \tag{13}$$

This set of equations have non-zero solution when the energy $E$ satisfies the implicit equation:

$$\begin{aligned} (1 + q\exp i\sigma_e)(1 + q\exp(-i\sigma_h)) \\ +p^2 \exp i(\sigma_e - \sigma_h) = 0 \end{aligned} \tag{14}$$

In the case where the bands are disconnected ($p = 0$), Eq. (14) can be factorized and reduces simply to $1 + \exp(i\sigma_e) = 0$ or $1 + \exp(-i\sigma_h) = 0$, which corresponds to the two independent sets of discrete energy levels given by Eq. (1). In general Eq. (14) can be solved numerically for $p \neq 0$: the field dependence of the LLs energy is plotted in Figs. 6 and 7 for $q$=0.6 and for 2 different sets of effective masses. In the case where $p \neq 0$, gaps open at the former LL intersections, and the structure of the two bands is modified. Alike in the case where $p = 0$, a quasi-hole and a quasi-electron band can be defined. Indeed, increasing the magnetic field, levels that go upwards above the Fermi energy $E_F(b)$ (see diamond symbol lines) and downwards below $E_F(b)$ represent quasi-electron and quasi-hole bands, respectively. At zero temperature, the compensation condition $N_e = N_h$ is replaced by the condition that the lower quasi-hole band is filled completely, the upper electron-band being empty. The two bands are therefore always separated by the chemical potential energy, as shown in Figs. 6 and 7. As the magnetic field decreases, the field-dependent Landau levels near the Fermi energy become flatter since the levels of each band do not intersect the Fermi level. In the case where $q = 0$ ($p = 1$), the quasiparticles tunnel directly through the 2 bands at each revolution, and the exact solution of Eq. (14) is given by the set of LLs:

$$\begin{aligned} E_{eh}(q = 0, n) &= E_F - b\frac{C_e C_h}{C_e + C_h}(n + \frac{1}{2}) \\ &= \frac{C_e}{C_e + C_h} E_h(n) \end{aligned} \tag{15}$$

with $n \geq 0$. Within the semi-classical approach, the cross-section area of the FS corresponding to this inverted parabolic quasi-hole band, which is completely filled, is zero. Since it is proportional to the frequency of the oscillations, there are no oscillations at $q = 0$. This simple feature is in line with the prediction of the semi-classical model for two compensated orbits, keeping in mind that the area of these orbits has opposite signs[3].

We assume that $C_h = C_e p_0/q_0$ where $p_0$ and $q_0$ are coprime integers[5,10]. Indeed, it is useful, also for computing time reasons, to approximate any real value of $C_h/C_e$ by a close rational ratio since in this case the spectrum (14) is periodic in energy, with periodicity $T_E = C_e b p_0$

In order to estimate the total free energy in the general case, it is necessary to solve numerically Eq. 14. We assume that $C_h = C_e p_0/q_0$ where $p_0$ and $q_0$ are coprime integers[5,10]. Indeed, it is useful, also for computing time reasons, to approximate any real value of $C_h/C_e$ by a

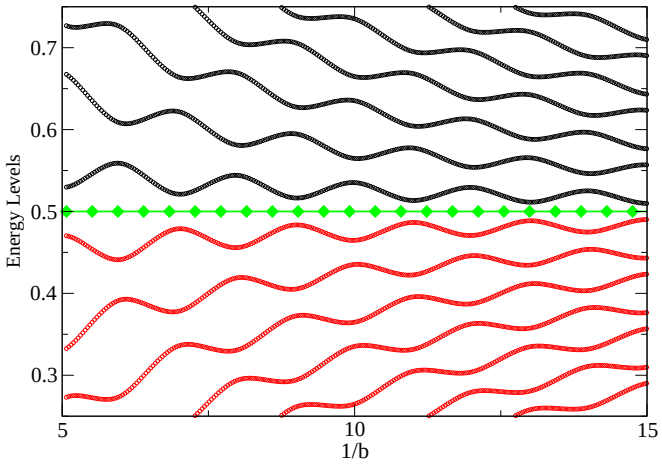


FIG. 7: (color online) Energy levels for a reflection amplitude $q = 0.6$, $\Delta = 1$, $m_e^* = m_h^* = 1$. Levels that belong to a quasi-electron band above the Fermi energy located at $E_F(b)$=0.5 (diamond symbols, green line) can be distinguished from levels that belong to a quasi-hole band (red lines). The 2 bands are fully symmetric with respect with the chemical potential energy.

close rational ratio since in this case the spectrum (14) is periodic in energy, with periodicity $T_E = C_e b p_0$ Within each interval $T_E$, there are exactly $p_0 + q_0$ discrete solutions (there is indeed conservation of the number of LLs when $q$ decreases from unity). By successive energy translations, it is then easy to reproduce all the spectrum. The GS energy $\Delta E_0$ given by Eq. (3) is however no more well defined, due to the mixing between electron and hole levels. Indeed, the GS energy should correspond to the sum of all the quasi-hole energies below the Fermi energy $E_F(b)$. These energies being not bounded by below, the GS energy is formally infinite. We propose to account numerically for this problem by introducing a cutoff function in the density of states with the necessary condition that the magnetization should not depend on variations of the cutoff parameters.

Given a set of LL energies $E_{eh}(q,n)$, $n = 0, \cdots, p_0 + q_0 - 1$, solutions of (14) in any energy interval of width $T_E$, we can introduce a cutoff function $\varphi_c(E)$ such as $\varphi_c(E) = 1$ for $E$ larger than a characteristic energy $E_c$ and equal to $\exp[-c(E - E_c)^{2\delta}]$ for $E \leq E_c$, where $\delta$ is any positive integer greater than 1 (we take $\delta = 4$ in the simulations which gives a very smooth cutoff function). This function has the required property of conserving the important physical properties near the Fermi surface and making in particular the GS energy finite. The LL density of states $\rho_c(E)$ takes the following form

$$\rho_c(E) = b \sum_{n=0}^{p_0+q_0-1} \sum_{k=-\infty}^{\infty} \varphi_c(E)\delta(E - E_{eh}(q,n) - kT_E)$$

Given $E_c$, the parameter $c$ is found to be solution of the equation of conservation at zero temperature:

$$\begin{aligned} N_{eh} &= \int_{-\infty}^{E_F(b)} dE \rho_c(E) \\ &= b \int_{-\infty}^{E_F(b)} dE \sum_{n=0}^{p_0+q_0-1} \sum_{k=-\infty}^{\infty} \varphi_c(E) \\ &\quad \delta(E - E_{eh}(q,n) - kT_E) \end{aligned} \tag{16}$$

where $N_{eh}$ is, as mentioned before, the total number of quasiparticles in the Canonical Ensemble. Once the parameter $c$ is obtained, we can define for example the GS energy $\Delta E_0$

$$\begin{aligned} \Delta E_0 &= b \int_{-\infty}^{E_F(b)} dE \sum_{n=0}^{p_0+q_0-1} \sum_{k=-\infty}^{\infty} \varphi_c(E) \\ &\quad E\delta(E - E_{eh}(q,n) - kT_E) \end{aligned} \tag{17}$$

or the free energy $\Delta F$

$$\begin{aligned} \Delta F &= -tb \int_{-\infty}^{\infty} dE \sum_{n=0}^{p_0+q_0-1} \sum_{k=-\infty}^{\infty} \varphi_c(E) \\ &\quad \log[1 + \exp\beta(\mu - E)]\delta(E - E_{eh}(q,n) - kT_E) \\ &+ N_{eh}\mu \end{aligned} \tag{18}$$

The potential $\mu(t,b)$ is calculated from Eq. (18) by extremizing the free energy $\partial\Delta F/\partial\mu = 0$, and compelling the magnetization $M_{osc} = -\partial\Delta F/\partial b$ to be independent of the parameter $E_c$ for $E_c$ far away from the chemical potential or at energies large compared to the Landau gap. We have checked, for different values of $E_c$ in units of $\Delta$, for example, $E_c = -1, -2, -4$, and for a large range of fields, that the resulting magnetization does not change. We choose $N_{eh}$, which is arbitrary, as a multiple of the characteristic zero field energy density $m_e^* + m_h^* = (C_e + C_h)/C_e C_h$ times the zero field Fermi energy $E_F$. For $E_c = -2$, we take in the following numerical simulations $N_{eh} = 8E_F(C_e + C_h)/C_e C_h$. Then, for each value of the field $b$, the parameter $c$ defined from Eq. (16) is unique. Also, in the case $q = 1$, the numerical solution for the magnetization is fully consistent with the results of the first section in absence of magnetic breakdown. In Fig. 8, the oscillations of the chemical potential $\mu(t,b)$ obviously decrease with $q$ until the total tunneling occurs where only orbits with frequency zero are allowed.

### A. Analytical amplitudes for small field

In this section, we extract the analytical expression for the first harmonics amplitude (corresponding to the frequency $F_0$) in the small $b/t$ regime, and compare it to the numerical results of the previous section. We first assume that the oscillations can be described by an effective free energy which is constructed by adding reflection

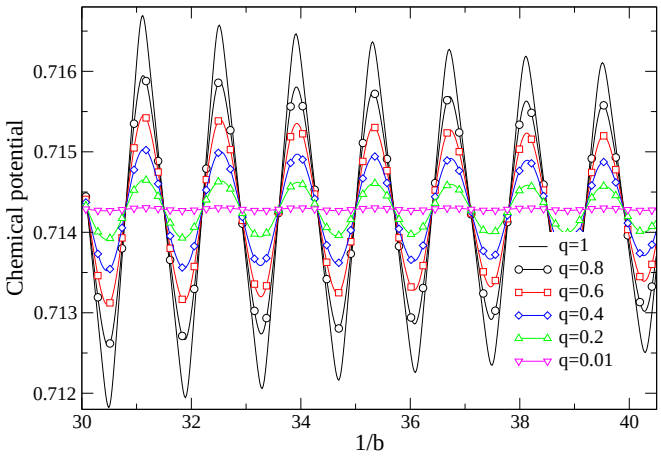


FIG. 8: (color online) Oscillations of the chemical potential at $t = 10^{-3}$ for different values of $q$; $\Delta = 1$, $m_e^* = 1$ and $m_h^* = 5/2$.

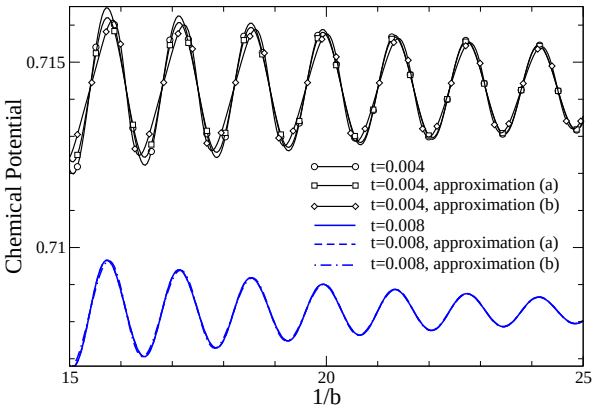


FIG. 9: (color online) Comparison between the numerical solution for $\mu$ (Eq. 18) with approximation (a) from Eq. (20), and (b) from Eq. (20) with $\mu$ in the sine functions replaced by $E_F$. $m_e^* = 1$ and $m_h^* = 5/2$, and $q = 0.6$. The 2 sets $t = 0.004$ and $t = 0.008$ are shifted along the vertical axis for clarity.

amplitudes $q^n$ to the temperature reduction factors in the expression of the Grand Potentials Eqs. 8 and 9, for orbits that circulate $n$ times around Fermi surfaces $S_e$ or $S_h$. In this approximation, it is indeed clear that the quasi-particles orbit the same surface if the field is small enough, and do not tunnel through the junction. The effective free energy can then be derived directly from Eqs. (8) and (9) as

$$\begin{aligned}\Delta F_{eff} &= \Omega_e - \Omega_h \simeq -\frac{\mu^2}{2C_e} - \frac{(\Delta-\mu)^2}{2C_h} \\ &+ \frac{b^2 C_e}{2}\sum_{n=1}^{\infty}\frac{(-q)^n}{\pi^2 n^2} R(nm_e^*)\cos(2\pi n\frac{\mu}{C_e b}) \\ &+ \frac{b^2 C_h}{2}\sum_{n=1}^{\infty}\frac{(-q)^n}{\pi^2 n^2} R(nm_h^*)\cos(2\pi n\frac{\Delta-\mu}{C_h b})\end{aligned} \quad (19)$$

and the chemical potential is derived as in Eq. 11

$$\begin{aligned}\mu &= E_F + \frac{b}{m_e^*+m_h^*}\sum_{n=1}^{\infty}\frac{(-q)^n}{\pi n}[R(nm_h^*)\sin(2\pi n\frac{\Delta-\mu}{C_h b}) \\ &- R(nm_e^*)\sin(2\pi n\frac{\mu}{C_e b})]\end{aligned} \quad (20)$$

Numerically, we can measure the deviations between this approximation and the numerical result $\mu = \partial\Delta F/\partial b$, where $\Delta F$ is defined by Eq. (18), for $m_e^* = 1$ and $m_h^* = 5/2$ (see Fig. 9), and find that Eq. (20) is valid for $b/t$ smaller than approximatively 12 (approximation (a)), and 8 in the case where $\mu$ is replaced by $E_F$ in the right hand side of Eq. (20) (approximation (b)), as in Eq. (12) for $q = 1$.

The complete derivation of the first harmonic amplitude is done in Appendix A. If we keep the dominant terms in Eq. (A7), which are those with the dominant reduction factor $R(m_{e(h)}^*)$, and discard the other exponentially small ones $R(nm_{e(h)}^*)$ for $n \geq 2$ or products $R(m_{e(h)}^*)^2$, we obtain

$$A_1 \simeq \frac{2F_0}{\pi} q\left\{\frac{R(m_e^*)}{m_e^*}\frac{J_1(\alpha_e)}{\alpha_e} + \frac{R(m_h^*)}{m_h^*}\frac{J_1(\alpha_h)}{\alpha_h}\right\} \quad (21)$$

where $\alpha_{e(h)} = 2m_{e(h)}^* q(R(m_e^*) - R(m_h^*))/(m_e^* + m_h^*)$ as defined in Appendix A, and $J_1$ is the Bessel function of order 1. In the limit where $\alpha_{e(h)}$ are small, the functions $2J_1(\alpha_{e(h)})/\alpha_{e(h)}$ are very close to unity and we recover the LK formula:

$$A_1^{LK} \simeq \frac{F_0}{\pi} q\left\{\frac{R(m_e^*)}{m_e^*} + \frac{R(m_h^*)}{m_h^*}\right\} \quad (22)$$

For example, for $q = 0.6$, $m_e^* = 1$ and $m_h^* = 5/2$, $\alpha_e$ vanishes when $b/t$ is either large or small, $\alpha_e$ being always less than 0.2 elsewhere. At this extremum value, the function $2J(x)/x$ is approximatively equal to 0.995. Therefore we do not expect, as in the case $q = 1$, a significant deviation from the LK formula at small $b/t$, as it can be seen in Fig. 10 in this range of fields for different values of $q$ strongly different from unity.

### B. LK formula for large field

In the large $b/t$ limit, the previous approximation is no more valid (the reduction factors are close to unity). We show hereafter that there are an infinite number of orbits contributing to the frequency $F_0$. These orbits, which are described in details in Appendix B, have large effective masses $m_e(n) = (n+1)m_e^* + nm_h^*$ or $m_h(n) = nm_e^* + (n+1)m_h^*$, where $n$ is a positive integer. Their contribution to

the total amplitude are therefore negligible at low field (or high temperature) since their reduction factors are exponentially small. An example of orbit of mass $m_e(1)$ contributing to frequency $F_0$ is shown in figure 11.

We can however compute the exact amplitude $A_1$ within the LK theory, and show that there is no discernible difference with the numerical solution of Eq. (18) in the Canonical Ensemble.

At low fields, the first harmonics amplitude $A_1$ contains the contribution of the 2 single orbits of mass $m_e^*$ and $m_h^*$, as in Eq. (22). At higher fields, we can replace the previous quantity by an exact expression

$$A_1^{LK} = \frac{F_0}{\pi}(T_e + T_h) \tag{23}$$

where the amplitudes $T_{e(h)}$ includes all the orbits that contribute to the first harmonics

$$T_{e(h)} = \frac{q}{m^*_{e(h)}} R(m^*_{e(h)}) + \sum_{n=1}^{\infty} \frac{t_{e(h)}(n)}{m_{e(h)}(n)} R(m_{e(h)}(n)) \tag{24}$$

The combinatorial coefficients $t_{e(h)}(n)$ defining the total amplitude for nonequivalent orbits of mass $m_{e(h)}(n)$ are computed in Appendix B. By definition, we set $t_{e(h)}(0) = q$. For comparison, we have solved numerically the magnetization from Eq. (18) for different values of $q$ and extracted the first harmonics $A_1$ from Fourier analysis. In Fig. 10 the amplitude of the first harmonics $A_1$ is plotted versus $b/t$ for $q = 0.6, 0.8, 0.98$ and 1 (symbols). Since $q$ depends on $b$ through the Chambers formula, these plots should merely be regarded as the temperature dependence of $A_1$ at a given magnetic field value. The data are compared to the predictions of the LK theory (solid lines) given by Eqs. (23), (24) and (B5), for $m_e^* = 1$ and $m_h^* = 5/2$. The deviations with the LK formula are negligible in all the $b/t$ range explored, whatever the $q$ value. In particular, the contributions of the higher mass orbits which become important in the large field range are still well described by the LK formula.

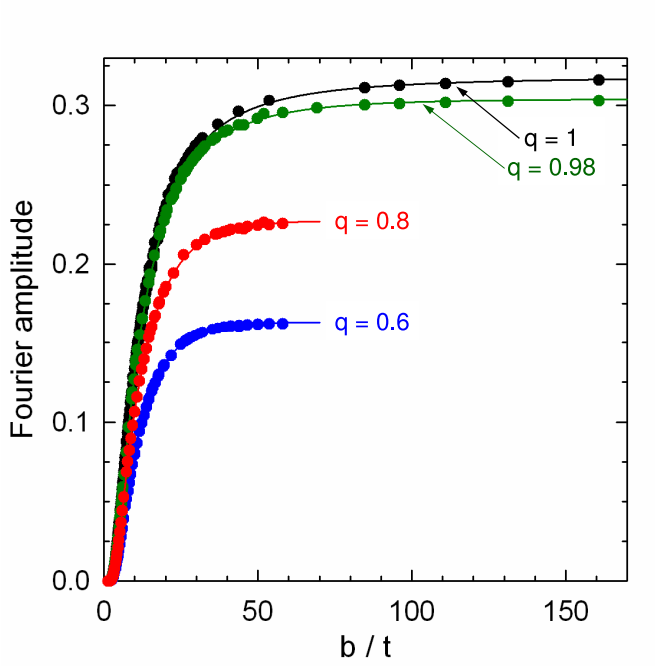


FIG. 10: (color online) First harmonics amplitude $A_1$ for different values of $q$; $\Delta = 1$, $m_e^* = 1$ and $m_h^* = 5/2$. The filled circle symbols represent the numerical analysis from the free energy expression (18), and the lines represent the LK formula (23, 24), with elements $t_{e(h)}(n)$ of Eq.(B10) computed up to $n = 10$ from Eq. (B5).

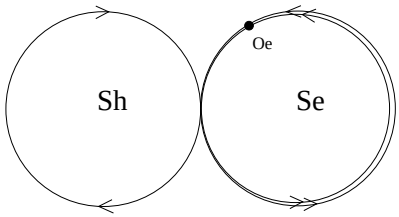


FIG. 11: Example of orbit contributing to first harmonics $F_0$. The effective mass here is $m_e(1) = 2m_e^* + m_h^*$. This orbit can be represented by the operator $\hat{Q}_e\hat{P}\hat{P}$ or $\hat{P}\hat{P}\hat{Q}_e$ (see Appendix B for details). The point $O_e$ on surface $S_e$ is crossed twice by the trajectory.

## VI. SUMMARY AND CONCLUSION

The field-dependent chemical potential oscillations in FS composed of two compensated electron and hole orbits is strongly damped when compared to the case of a FS with only electronic orbits[7–10]. It is even suppressed in the case where the effective mass of electron ($m_e^*$) and hole ($m_h^*$) band are the same (assuming the relaxation times $t^*_{e(h)}$ are either identical or negligibly small). In addition, the LK formula accounts for the field and temperature dependence of the first harmonic's dHvA oscillations amplitude in all cases. As for the amplitude of the second harmonics, it is accounted for by the LK formula, provided $m_e^*$ and $m_h^*$ are not strongly different. Besides, as MB develops, the chemical potential oscillations are further damped and the previous conclusion on the LK validity still holds for the amplitude of the first harmonic. In this case, as well as in the general case of compensated electron-hole orbits, the contributions of an infinite number of orbits to the main frequency become relevant at high fields, due to the existence of closed trajectories in the FBZ which have zero frequency and make the expression of the LK amplitude rather complex. Within the FS topology that we have considered here, we have demonstrated that it can nevertheless be computed exactly. We expect these additional "zero frequency" orbits to be reminiscent in other systems as well.

Finally, it should be noticed that the Landau energy spectrum of 1D and 2D periodic networks of electron-hole compensated orbits (see Figs. 1(b) and (a), respectively), is likely a set of Landau bands rather than discrete Landau levels as observed in Figs. 6 and 7. This feature could induce a MB-induced modulation of the density of states, as observed in non-compensated networks,[4–6] and hence frequency combinations in dHvA oscillatory spectra. In that respect, the reported method for solving Eq. 14 can be used for the study of such orbits networks.

## APPENDIX A

From Eq. (20), we can define the periodic function

$$G(x) = \sum_{n=1}^{\infty} \frac{(-q)^n}{\pi n}[R(nm_h^*) - R(nm_e^*)]\sin(2\pi n F_0 x) \quad \text{(A1)}$$

where $x = 1/b$. The chemical potential Eq. (20) becomes $\mu = E_F + bG(x)/(m_e^* + m_h^*)$. Replacing $\mu$ in (19) by the previous expression, we compute the oscillating part of the magnetization $M_{osc} = -\partial \Delta F_{eff}/\partial b = x^2 \partial \Delta F_{eff}/\partial x$:

$$\begin{aligned} M_{osc} &\approx -\frac{C_e C_h}{(C_e + C_h)} G(x) G'(x) \quad \text{(A2)} \\ &+ \frac{1}{2}\sum_{n=1}^{\infty} \frac{(-q)^n}{\pi^2 n^2}\left[ C_e R(nm_e^*) \frac{\partial}{\partial x} \Re \exp(2i\pi n \frac{\mu}{C_e} x) \right. \\ &+ \left. C_h R(nm_h^*) \frac{\partial}{\partial x} \Re \exp(2i\pi n \frac{\mu - \Delta}{C_h} x) \right] \end{aligned}$$

We also define the Fourier coefficients $B_{e(h)}(n,m)$ as

$$e^{2i\pi n w_{e(h)} G(x)} = \sum_{m=-\infty}^{+\infty} B_{e(h)}(n,m) e^{2i\pi m F_0 x} \quad \text{(A3)}$$

where $w_{e(h)} = C_{h(e)}/(C_e + C_h)$. Then, we perform the derivatives in expression (A2) by noticing for example that

$$\begin{aligned} &\frac{\partial}{\partial x} \Re \exp(2i\pi n \frac{\mu}{C_e} x) = \Re \left[ \sum_{m=-\infty}^{+\infty} B_e(n,m) \right. \\ &\left. \times 2i\pi(m+n) F_0 \exp(2i\pi(m+n)F_0 x) \right] \quad \text{(A4)} \end{aligned}$$

and

$$\begin{aligned} &\frac{\partial}{\partial x} \Re \exp(2i\pi n \frac{\mu - \Delta}{C_h} x) = \Re \left[ \sum_{m=-\infty}^{+\infty} B_h(n,m) \right. \\ &\left. \times 2i\pi(m-n) F_0 \exp(2i\pi(m-n)F_0 x) \right] \quad \text{(A5)} \end{aligned}$$

For extracting the first amplitude, we select the integers such as $m + n = \pm 1$ in (A4) and $m - n = \pm 1$ in (A5). In the product $G(x)G'(x)$ of expression (A2), the terms can be rearranged noticing that $\cos(2\pi m F_0 x)\sin(2\pi n F_0 x) = [\sin(2\pi(n+m)F_0 x) + \sin(2\pi(n-m)F_0 x)]/2$ with $m, n \geq 1$. For the first harmonic, only terms $n - m = \pm 1$ contribute. A further approximation is to keep the first term of the series (A1), i.e. $G(x) \approx -q(R(m_h^*) - R(m_e^*))\sin(2\pi F_0 x)/\pi$, in (A3), so that the coefficients $B_{e(h)}(n,m)$ can be computed exactly, from the explicit relation

$$\begin{aligned} &\exp\left[2inw_{e(h)} q(R(m_e^*) - R(m_h^*))\sin(2\pi F_0 x)\right] = \\ &\sum_{m=-\infty}^{\infty} J_m(n\alpha_{e(h)}) \exp(2i\pi m F_0 x) \quad \text{(A6)} \end{aligned}$$

where $J_m$ is the Bessel function of order $m$ and $\alpha_{e(h)} = 2w_{e(h)} q(R(m_e^*) - R(m_h^*))$. In this case it is easy to identify $B_{e(h)}(n,m) = J_m(n\alpha_{e(h)})$. After some algebra, we find that the amplitude $A_1$ for the first harmonic $F_0$ is given by the expression, in the large $t/b$ limit

$$\begin{aligned} \frac{\pi A_1}{F_0} &\approx \sum_{n=1}^{\infty} 2\frac{(-q)^n}{n}\left\{ (-1)^n C_e R(nm_e^*) \frac{J_n(n\alpha_e)}{n\alpha_e} \right. \\ &- \left. C_h R(nm_h^*) \frac{J_n(n\alpha_h)}{n\alpha_h} \right\} + \frac{C_e C_h}{C_e + C_h} \times \\ &\sum_{n=1}^{\infty} \frac{1}{n}[R(nm_h^*) - R(nm_e^*)] \times \quad \text{(A7)} \\ &\left\{ [R((n-1)m_h^*) - R((n-1)m_e^*)] q^{2n-1} \right. \\ &\left. - [R((n+1)m_h^*) - R((n+1)m_e^*)] q^{2n+1} \right\} \end{aligned}$$

## APPENDIX B

In this appendix, we compute the amplitude of the first hamonics in the LK theory for any given reflection amplitude $q$. In the lowest approximation, the contribution to the amplitude is given by one single orbit around the electron or hole band (see Fig. 5). Each contributes with a mass equal to $m_e^* = 1/C_e$ and $m_h^* = 1/C_h$ respectively and a reflection amplitude $q$ at the junction point. At finite temperature, we add a reduction factor $R(m_e^*)$ or $R(m_h^*)$ so that we obtain (with a $F_0$ factor overall) Eq. (22).

However, there are other contributions to the $F_0$ harmonics, coming from more complex orbits. For example in Fig. 11, from a starting point $O_e$ near the junction on the Fermi surface $S_e$, we can reach the junction point and go through to the other band $S_h$, then complete an entire orbit and come back through the same junction to the band $S_e$, and finally perform 2 orbits around $S_e$ until we reach $O_e$ again. The frequency will be proportional to $2S_e - S_h$. For a compensated system, this

frequency is just $F_0$ since $S_e = S_h$. The total mass is however proportional to the derivative of $2S_e - S_h$ with respect to the energy, which is $2m_e^* + m_h^*$ (the derivative of $S_h = 2\pi m_h^*(\Delta - E)$ is indeed negative). Therefore we should take into account all possible trajectories. This can be done exactly by summing up all the contributions for a given mass $m_e(n) = (n+1)m_e^* + nm_h^*$ $(n \geq 0)$. As before we start from a point $O_e$ $(O_h)$ on the surface $S_e$ $(S_h)$ and turn until we reach the junction. Here we note $\hat{Q}_e$ $(\hat{Q}_h)$ the reflection operator which keep the quasiparticle on the surface $S_e$ with amplitude $q$ ($S_h$ respectively), and $\hat{P}$ the operator which take the quasiparticle through the junction (with amplitude $ip$). Their electron-hole representations are given by the matrices:

$$\hat{Q}_e = \hat{Q}_h = \begin{pmatrix} q & 0 \\ 0 & q \end{pmatrix}, \quad \hat{P} = \begin{pmatrix} 0 & ip \\ ip & 0 \end{pmatrix} \tag{B1}$$

In the simplest case, the orbit is described only by the operator or graph $\hat{Q}_e$, whereas in the second example, the orbit is described by the graph $\hat{P}\hat{P}\hat{Q}_e$. The orbit $\hat{Q}_e\hat{P}\hat{P}$ is equivalent and has the same mass $2m_e^* + m_h^*$. Indeed, the orbit goes trough the same point $O_e$ twice, and therefore there are 2 different ways of writing the graph above, depending on which branch of the orbit we place the point $O_e$. Equivalent graphs are described by a cyclic permutation of their operator elements. We also observe that multiple orbits $(\hat{P}\hat{P})^n$ have zero frequency and mass $n(m_e^*+m_h^*)$. We will note in the following $t_e(n)$ $(t_h(n))$ the sums of the amplitudes of all the trajectories with the same mass $m_e(n)$ $(m_h(n) = nm_e^* + (n+1)m_h^*$ respectively), which are constructed starting from an arbitrary point $O_e$ (or $O_h$ respectively). $T_e$ $(T_h)$ will be the total amplitude for the frequency $F_0$ $(-F_0)$ starting from point $O_e$ $(O_h)$ on the surface $S_e$ $(S_h)$, see Eqs. (23,24)

$T_h$ is computed in the same way as $T_e$ by replacing the label $e$ in all the quantities by $h$. For equal masses $m_e^* = m_h^*$, we have clearly $T_e = T_h$. For example, the orbits and amplitudes contributing to the mass $m_e(1) = 2m_e^* + m_h^*$ are

$$\hat{P}\hat{P}\hat{Q}_e \sim \hat{Q}_e\hat{P}\hat{P} \rightarrow (-p^2)q,$$

This gives $t_e(1) = (-p^2)q$. The 2 operators above correspond to the same graph by a cyclic permutation of their elements $\hat{P}\hat{P}$ and $\hat{Q}_e$ and the sign $\sim$ is understood as an equivalence between identical graphs. In the next case, for the mass $m_e(2) = 3m_e^* + 2m_h^*$ we have the possibilities

$$\hat{P}\hat{Q}_h\hat{P}\hat{Q}_e^2 \sim \hat{Q}_e\hat{P}\hat{Q}_h\hat{P}\hat{Q}_e \sim \hat{Q}_e^2\hat{P}\hat{Q}_h\hat{P} \rightarrow (-p^2)q^3,$$
$$\hat{P}\hat{P}\hat{P}\hat{P}\hat{Q}_e \sim \hat{P}\hat{P}\hat{Q}_e\hat{P}\hat{P} \sim \hat{Q}_e\hat{P}\hat{P}\hat{P}\hat{P} \rightarrow (-p^2)^2 q$$

we obtain $t_e(2) = (-p^2q^3 + p^4q)$. In the general case, we can construct all the possible orbits that contribute to the mass $m_e(n)$ by representing them as multiple products of elementary operators

$$\hat{Q}_e^{n_1}\hat{P}\hat{Q}_h^{m_1}\hat{P}\hat{Q}_e^{n_2}\hat{P}\hat{Q}_h^{m_2}\hat{P}..\hat{Q}_e^{n_k}\hat{P}\hat{Q}_h^{m_k}\hat{P} \tag{B2}$$

where $n_i \geq 0$ and $m_i \geq 0$ are positive integers. The constraints imposed by the mass on theses integers and $k$ are

$$\sum_{i=1}^{k} n_i = n - k + 1, \; \sum_{i=1}^{k} m_i = n - k, \; 1 \leq k \leq n \tag{B3}$$

There are also $k$ cyclic permutations of the graph (B2) above, corresponding to moving elements $\hat{Q}_e^{n_i}\hat{P}\hat{Q}_h^{m_i}\hat{P}$ to the right or to the left. For example, an equivalent graph would be

$$\hat{Q}_e^{n_2}\hat{P}\hat{Q}_h^{m_2}\hat{P}..\hat{Q}_e^{n_k}\hat{P}\hat{Q}_h^{m_k}\hat{P}\hat{Q}_e^{n_1}\hat{P}\hat{Q}_h^{m_1}\hat{P} \tag{B4}$$

The total amplitude $t_e(n)$ for a given $n$ can be written as

$$t_e(n) \; = \; \sum_{k=1}^{n} c_{n,k}(-p^2)^k q^{2(n-k)+1} \tag{B5}$$

where the coefficients $c_{n,k}$ enumerate the number of all nonequivalent graphs having the same mass, up to cyclic permutations. It corresponds to all possible sets of $n_i$ and $m_i$ representing graphs (B2) with the constraint (B3), divided by the number of cyclic permutations $k$. The total amplitude $t_e(n)$ can be written more precisely as

$$t_e(n) \; = \; \sum_{k=1}^{n} \sum_{n_i, m_i \geq 0} q^{\sum_{i=1}^{k} n_i + \sum_{i=1}^{k} m_i}(-p^2)^k \times \frac{1}{k}\delta_{\sum_{i=1}^{k} n_i, n-k+1}\delta_{\sum_{i=1}^{k} m_i, n-k} \tag{B6}$$

The Kronecker functions $\delta_{k,0}$ can be represented by integrals $\delta_{k,0} = \int_0^1 \exp(2i\pi kx)dx = \oint dz/(2i\pi z) \times z^k$, and the last expression becomes

$$t_e(n) = \sum_{k=1}^{n} \frac{(-p^2)^k}{k} \oint \frac{dz}{2i\pi z} \oint \frac{dz'}{2i\pi z'} \left(\prod_{i=1}^{k} \sum_{n_i=0}^{\infty} q^{n_i} z^{n_i}\right) z^{k-n-1} \left(\prod_{i=1}^{k} \sum_{m_i=0}^{\infty} q^{m_i} z'^{m_i}\right) z'^{k-n} \tag{B7}$$

Summing up the series, we obtain

$$t_e(n) \; = \; \sum_{k=1}^{n} \frac{(-p^2)^k}{k} \oint \frac{dz}{2i\pi} \frac{z^{k-n-2}}{(1-qz)^k} \oint \frac{dz'}{2i\pi} \frac{z'^{k-n-1}}{(1-qz')^k}$$

Applying the residue theorem, it is easy to show that

$$\oint \frac{dz}{2i\pi} \frac{z^{k-n-2}}{(1-qz)^k} = \binom{n}{k-1} q^{n-k+1} \tag{B8}$$

and

$$\oint \frac{dz'}{2i\pi} \frac{z'^{k-n-1}}{(1-qz')^k} = \binom{n-1}{k-1} q^{n-k} \tag{B9}$$

where $\binom{n}{k} = n!/k!(n-k)!$ are the binomial coefficients. We obtain finally

$$c_{n,k} = \frac{1}{k} \binom{n}{k-1} \binom{n-1}{k-1} \tag{B10}$$

The values of the coefficients $c_{n,k}$ up to $n = 7$ are given in Table 1.

TABLE I: Values of the coefficients $c_{n,k}$ which represent the number of non-equivalent orbits for a given mass $(n+1)m^*_{e(h)} + nm^*_{h(e)}$ with $2k$ breakdowns, $1 \le k \le n$.

| $n \backslash k$ | 1 | 2 | 3 | 4 | 5 | 6 | 7 | Mass |
|---|---|---|---|---|---|---|---|---|
| 1 | 1 | | | | | | | $2m^*_{e(h)} + m^*_{h(e)}$ |
| 2 | 1 | 1 | | | | | | $3m^*_{e(h)} + 2m^*_{h(e)}$ |
| 3 | 1 | 3 | 1 | | | | | $4m^*_{e(h)} + 3m^*_{h(e)}$ |
| 4 | 1 | 6 | 6 | 1 | | | | $5m^*_{e(h)} + 4m^*_{h(e)}$ |
| 5 | 1 | 10 | 20 | 10 | 1 | | | $6m^*_{e(h)} + 5m^*_{h(e)}$ |
| 6 | 1 | 15 | 50 | 50 | 15 | 1 | | $7m^*_{e(h)} + 6m^*_{h(e)}$ |
| 7 | 1 | 21 | 105 | 175 | 105 | 21 | 1 | $8m^*_{e(h)} + 7m^*_{h(e)}$ |

We also observe by symmetry that $t_h(n)$ is equal to $t_e(n)$ since this geometric coefficient does not depend explicitely on masses.


* Electronic address: fortin@lpt1.u-strasbg.fr
† Electronic address: audouard@lncmp.org



[1] A. Pippard, Proc. R. Soc. London **A 270**, 1 (1962).
[2] For a review, see M. Kartsovnik, Chem. Rev. **104** 5737 (2004) and references therein.
[3] L. M. Falicov and H. Stachowiak, Phys. Rev. **147**, 505 (1966).
[4] P. S. Sandhu, J. H. Kim, and J. S. Brooks, Phys. Rev. B **56**, 11566 (1997).
[5] J.-Y. Fortin and T. Ziman, Phys. Rev. Lett. **80**, 3117 (1998).
[6] V. M. Gvozdikov, Y. V. Pershin, E. Steep, A. G. M. Jansen, and P. Wyder, Phys. Rev. B **65**, 165102 (2002).
[7] A. S. Alexandrov and A. M. Bratkovsky, Phys. Rev. Lett. **76**, 1308 (1996).
[8] T. Champel, Phys. Rev. B **65**, 153403 (2002).
[9] K. Kishigi and Y. Hasegawa, Phys. Rev. B **65**, 205405 (2002).
[10] J.-Y. Fortin, E. Perez, and A. Audouard, Phys. Rev. B **71**, 155101 (2005).
[11] L. F. Veiros and E. Canadell, J. Phys. I France **4**, 939 (1994).
[12] C. Proust, A. Audouard, L. Brossard, S. I. Pesotskii, R. B. Lyubovskiĭ, and R. N. Lyubovskaya, Phys. Rev. B **65**, 155106 (2002).
[13] D. Vignolles, A. Audouard, L. Brossard, S. I. Pesotskii, R. B. Lyubovskiĭ, M. Nardone, E. Haanappel, and R. N. Lyubovskaya, Eur. Phys. J. B **31**, 53 (2003).
[14] A. Audouard, D. Vignolles, E. Haanappel, I. Sheikin, R. B. Lyubovskiĭ, and R. N. Lyubovskaya, Europhys. Lett. **71**, 783 (2005).
[15] R. Rousseau, M. Gener, and E. Canadell, Adv. Func. Mater. **14**, 201 (2004).
[16] A. D. Dubrovskii, N. G. Spitsina, L. I. Buravov, G. V. Shilov, E. B. Dyachenko, O. A. and. Yagubskii, V. N. Laukhin, and E. Canadell, J. Mater. Chem. **15**, 1248 (2005).
[17] T. G. Prokhorova, S. S. Khasanov, L. V. Zorina, L. I. Buravov, V. A. Tkacheva, A. A. Baskakov, R. B. Morgunov, M. Gener, E. Canadell, R. P. Shibaeva, et al., Adv. Funct. Mater. **13**, 403 (2003).
[18] P. M. Grant, Phys. Rev. Lett. **50**, 1005 (1983).
[19] D. Vignolles, A. Audouard, M. Nardone, L. Brossard, S. Bouguessa, and J.-M. Fabre, Phys. Rev. B **71**, 020404 (2005).
[20] R. N. Lyubovskaia, O. A. Dyachenko, V. V. Gritsenko, S. G. Mkoyan, L. O. Atovmyan, R. B. Lyubovskii, V. N. Laukhin, A. V. Zvarykina, and A. G. Khomenko, Synth. Metals **42**, 1907 (1991).
[21] D. Shoenberg, *Magnetic Oscillations in Metals* (Cambridge University Press, Cambridge, England, 1984).
[22] A. Kosevich and I. Lifschitz, Sov. Phys. JETP **2**, 646 (1956).
[23] The two electronic orbits considered in Fig. 1 have different frequencies, namely $f_0$ / $f_1$ = 2 / 3. In the case where $f_0 = f_1$, the chemical potential oscillations are even larger than reported in Fig. 1 since the field-dependent contributions of the two orbits are in phase.
[24] V. M. Gvozdikov and M. Taut, Phys. Rev. B **75**, 155436 (2007).
[25] R. Chambers, Proc. Phys. Soc. **65**, 458 (1952).
[26] A. Slutskin and A. Kadigrobov, Sov. Phys. Solid State **9**, 138 (1967).